NASA / TM—1998-107529

Comparison of Graphite Fabric Reinforced PMR–15 and Avimid N Composites After Long Term Isothermal Aging at Various Temperatures

Kenneth J. Bowles
Lewis Research Center, Cleveland, Ohio

Linda McCorkle and Linda Ingrahm
Gilcrest Corporation, Cleveland, Ohio

February 1998

The NASA STI Program Office . . . in Profile

Since its founding, NASA has been dedicated to the advancement of aeronautics and space science. The NASA Scientific and Technical Information (STI) Program Office plays a key part in helping NASA maintain this important role.

The NASA STI Program Office is operated by Langley Research Center, the Lead Center for NASA's scientific and technical information. The NASA STI Program Office provides access to the NASA STI Database, the largest collection of aeronautical and space science STI in the world. The Program Office is also NASA's institutional mechanism for disseminating the results of its research and development activities. These results are published by NASA in the NASA STI Report Series, which includes the following report types:

- TECHNICAL PUBLICATION. Reports of completed research or a major significant phase of research that present the results of NASA programs and include extensive data or theoretical analysis. Includes compilations of significant scientific and technical data and information deemed to be of continuing reference value. NASA's counterpart of peer-reviewed formal professional papers but has less stringent limitations on manuscript length and extent of graphic presentations.

- TECHNICAL MEMORANDUM. Scientific and technical findings that are preliminary or of specialized interest, e.g., quick release reports, working papers, and bibliographies that contain minimal annotation. Does not contain extensive analysis.

- CONTRACTOR REPORT. Scientific and technical findings by NASA-sponsored contractors and grantees.

- CONFERENCE PUBLICATION. Collected papers from scientific and technical conferences, symposia, seminars, or other meetings sponsored or cosponsored by NASA.

- SPECIAL PUBLICATION. Scientific, technical, or historical information from NASA programs, projects, and missions, often concerned with subjects having substantial public interest.

- TECHNICAL TRANSLATION. English-language translations of foreign scientific and technical material pertinent to NASA's mission.

Specialized services that complement the STI Program Office's diverse offerings include creating custom thesauri, building customized data bases, organizing and publishing research results . . . even providing videos.

For more information about the NASA STI Program Office, see the following:

- Access the NASA STI Program Home Page at ***http://www.sti.nasa.gov***

- E-mail your question via the Internet to help@sti.nasa.gov

- Fax your question to the NASA Access Help Desk at (301) 621-0134

- Telephone the NASA Access Help Desk at (301) 621-0390

- Write to:
  NASA Access Help Desk
  NASA Center for AeroSpace Information
  800 Elkridge Landing Road
  Linthicum Heights, MD 21090-2934

NASA / TM—1998-107529

Comparison of Graphite Fabric Reinforced PMR–15 and Avimid N Composites After Long Term Isothermal Aging at Various Temperatures

Kenneth J. Bowles
Lewis Research Center, Cleveland, Ohio

Linda McCorkle and Linda Ingrahm
Gilcrest Corporation, Cleveland, Ohio

National Aeronautics and
Space Administration

Lewis Research Center

February 1998

Trade names or manufacturers' names are used in this report for identification only. This usage does not constitute an official endorsement, either expressed or implied, by the National Aeronautics and Space Administration.

Available from

NASA Center for Aerospace Information
800 Elkridge Landing Road
Linthicum Heights, MD 21090-2934
Price Code: A03

National Technical Information Service
5287 Port Royal Road
Springfield, VA 22100
Price Code: A03

Comparison of Graphite-Fabric-Reinforced PMR–15 and Avimid N Composites After Long-Term Isothermal Aging at Various Temperatures

Kenneth J. Bowles
National Aeronautics and Space Administration
Lewis Research Center
Cleveland, Ohio 44135

Linda McCorkle and Linda Ingrahm
Gilcrest Corporation
Cleveland, Ohio 44135

INTRODUCTION

Extensive effort is currently being expended to demonstrate the feasibility of using high-performance, polymer-matrix composites as engine structural materials over the expected operating lifetime of the aircraft, which can extend from 18 000 to 30 000 hr. The goal is to develop light-weight, high-strength, and high-modulus materials for use in higher temperature sections of advanced 21st century aircraft propulsion systems. To accomplish this goal, it is necessary to pursue the development of thermal and mechanical durability models for graphite-fiber-reinforced, polymer-matrix composites.

Numerous investigations have been reported regarding the thermo-oxidative stability (TOS) of the polyimide PMR–15 (1–5). A significant amount of this work has been directed at edge and geometry effects, reinforcement fiber influences, and empirical modeling of high-temperature weight loss behavior. It is yet to be determined if the information obtained from the PMR–15 composite tests is applicable to other polyimide-matrix composites.

The condensation-curing polymer Avimid N is another advanced composite material often considered for structural applications at high temperatures. Avimid N has better thermo-oxidative stability than PMR–15 (6), but the latter is more easily processed. The most comprehensive study of the thermo-oxidative stability of Avimid N neat resin and composites at 371 °C is found in Salin and Seferis (7). The purposes of the work described herein were to compare the thermal aging behavior of

these two matrix polymers and to determine the reasons for and the consequences of the difference in thermal durability. These results might be of some use in improving future polymer development through the incorporation of the desirable characteristics of both polyimides.

MATERIALS

The materials used in this study were PMR–15 polyimide composites reinforced with T650–35, 24 by 23, eight-harness satin carbon fiber fabric and Avimid N composites reinforced with the same carbon fabric. The two matrix polymers (PMR–15 and Avimid N) differ in their processing characteristics. The Avimid N polymer undergoes curing by a condensation reaction in which volatile reaction products, such as water and alcohols, are produced (8). During composite processing these byproducts can cause blistering and void formation. The solvent used to prepare the impregnating solution is a mixture of *n*-methyl pyrollidone (NMP) and ethanol (9). NMP has a very low vapor pressure; and intricate, time-consuming curing schedules must be used to expel the solvent in order to produce low-void composites. Voids were present in the Avimid composites used in this study.

Addition-curing polymers, such as PMR–15, undergo their final cure without producing these byproducts. They are cured in a two-step process in which the volatiles are removed in a lower temperature reaction (200 °C) that produces low-molecular-weight oligomers (8). These oligomers are then cross-linked at the final cure temperature of 316 °C. The nadic end cap, which controls the molecular weight, is also why the PMR–15 has a lower TOS than the condensation-curing Avimid N (8). The cross-linking of PMR–15 also allows a higher glass transition temperature T_G to be attained more easily for this addition-curing polymer.

The PMR–15 composites were fabricated by autoclave techniques at 316 °C. The cure was followed by a free-standing postcure in an air-circulating oven at 316 °C for 16 hr. All PMR–15 processing was done at the General Electric Aircraft Engine Plant in Evendale, Ohio. The specimen designations and nominal dimensions are presented in Table 1. The dimensions were selected to provide specimens with different ratios of molded surface areas (resin-rich areas adjacent to the vacuum bag containment materials) to cut surface areas. The percentage of cut surface areas varied from 2.7 to 89% of the total surface area. The specimen designations reflect the nominal percentage of

cut areas. The PMR–15 matrix material had void contents less than 2% and was free from delaminations. A typical photomicrograph of the PMR–15 material prior to aging is shown in Fig. 1. Some resin-rich areas are present between the tows.

One Avimid N specimen with 27% cut surface areas was aged at each temperature studied (204, 260, 288, 316, and 343 °C). The dimensions of the specimen, designated as AT–27, are also included in Table 1. (All the other specimens in Table 1 are PMR–15.) This specimen had nominally the same dimensions as the T–27 PMR–15 plate. The details of the composite processing are not available, since the work was done at the DuPont facilities. A typical photomicrograph of the Avimid N material prior to aging is presented in Fig. 2. It contained significant voids in the central portion of the laminates. The thicknesses at the void-free edges were less than those in the interior.

TEST PROCEDURES

Thermo-oxidative Stability

The composite specimens were aged in air-circulating ovens with a flow rate of 100 cm^3/min at 204, 260, 288, 316 and 343 °C. The specimens were removed from the ovens at regular intervals and placed in a desiccator where they cooled to room temperature. The specimens were not removed from the desiccator until they were ready to be weighed. The weights were recorded and the specimens were returned to the ovens. At scheduled times selected specimens were removed permanently from the ovens for various tests.

Dynamic Mechanical Analysis

Oxidation and thermal degradation of the graphite-fabric-reinforced PMR–15 composites can be correlated with changes in the stored shear modulus G' that occurred in the damaged layer located at the exposed surfaces of the aging specimens. As the layer grew, the G' and T_G values changed to reflect the chemical and physical changes taking place within the damaged layer. This phenomenon also occurred in the bulk (core) of the specimens. The glass transition temperature is commonly related to the degree of cross-linking in a polymer.

The dynamic measurements were made with rectangular test pieces and by using a Rheometrics RMS–800 rheological spectrometer. The test pieces were stressed in torsion across the specimen widths. The test pieces were 60 mm long, 10 mm wide, and 1 to 6 mm thick. They were mounted in grips separated to give a gage length of 45 mm. The two components of the complex shear modulus were measured as a function of temperature. A frequency of 1 Hz with an amplitude of 0.1% strain and a heating rate of 5 deg C/min were used. All specimens were dried in an air-circulating oven at 125 °C for 24 hr before testing. This time was sufficient to reduce the moisture content to very low values (9). The glass transition temperatures were determined by measuring the intersection of the two tangents to the G' curve where it changed slope as illustrated in Fig. 3.

Compression Tests

The compression testing was done at the Cincinnati Testing Laboratories in Forest Hills, Ohio, in accordance with the specifications in ASTM D–695M. Two exceptions to these specifications were made as noted later in the text. The test speed was 1.27 mm/min. Strain measurements were made with an extensometer. No end tabs were used. All specimens were conditioned at 125 °C for 16 hr before testing. The tests were run at 23.3 °C and a relative humidity of 50%.

Fiber and Void Content

The fiber contents of the composites were measured by acid digestion as described in ASTM D–3171. The void volume was calculated as the difference between the specific volume of a composite specimen, measured by the immersion technique as specified in ASTM 792, and the theoretical specific volume calculated from the acid digestion results. The densities of the PMR–15 polymer and fiber were taken to be 1.32 and 1.78 g/cm^3, respectively. The density of the Avimid N was taken as 1.4 g/cm^3 (7). The void percentage was the difference between the measured specific volume and the specific volume calculated from the digestion results divided by the measured specific volume and then multiplied by 100.

RESULTS

Thermo-oxidative Stability

Results of aging weight loss tests on some PMR–15 composites at 316 °C are presented in Fig. 4. The data for three thicknesses of panels with identical widths and lengths are shown to illustrate the effect of specimen volume (thickness) on the weight loss that results from exposure. The thickest specimen lost the lowest percentage of its original weight after aging at 316 °C. Therefore, only specimens of like dimensions can be directly compared on the basis of mass loss. Similar results were observed at the other temperatures.

The weight loss data for the PMR–15 composite T–27 and the Avimid N composite AT–27 at the five aging temperatures studied are compared in Fig. 5. During the initial aging period the weight losses for the PMR–15 composite increased rapidly (origin to point A), and then a linear rate with time was established for a significant period of time (point A to point B). In contrast, the data for the Avimid N composite monotonically increased at a slower initial rate (origin to point A) than did the PMR–15 composite. However, from point A to point B the linear slopes of the weight loss curves for both composites are similar if not identical. For both composite systems the slopes of the curves increase at point B, indicating an accelerated weight loss rate.

From these data three different mechanisms appear to control the TOS of the two composite systems. The shapes of the curves are similar for all aging temperatures studied. The main difference between the shapes and magnitudes of the two curves was the initial volume-dependent, rapid weight loss of the PMR–15 composites.

The magnitude of the initial rapid weight loss (up to point A in Fig. 5) varied with specimen volume for PMR–15 specimens aged at or above 288 °C as shown graphically in Fig. 6. At aging temperatures below 260 °C both volume and surface area contributed to initial weight loss.

Dynamic Mechanical Analysis

The types of specimens dynamically tested were the T–5 plate (more than 90% molded surface), the T–27 plate, the AT–27 plate, and the T–89 plate (almost 90% cut surface). The data for the 90% molded surface and the 90% cut surface differed significantly. Figure 7 shows typical

dynamic mechanical analysis (DMA) data generated from these two specimen types (T–5 and T–89) after aging at 316 °C for 1000 hr. The tan δ peak (where $\delta = G''/G'$) occurred at about the same temperature (400 °C) for both specimen types. The tan δ peak broadened and decreased only slightly for T–89. Before T_G both the G' and G'' curves were fairly flat for both specimen types but the values were somewhat lower for the T–89. The significant difference in the materials was the G' and G'' behavior above T_G. The peaking and extreme dropoff exhibited for the T–5 material (Fig. 7(a)) was absent in the data for the T–89 material (Fig. 7(b)). No decrease in shear modulus occurred at the higher aging temperatures. The data from an unaged T–89 specimen (Fig. 8) were similar to those for the T–5 specimen aged at 316 °C (Fig. 7(a)). Therefore, the change in dynamic shear modulus behavior was probably due to the aging process and not to geometric differences.

The T–89 specimens were narrow (2 mm), and the cut surfaces were sites of crack initiation as the aging of these specimens proceeded. Therefore, they were tested for crack penetration by a liquid. A drop of ethanol was placed on one cut surface; complete penetration was indicated by the presence of ethanol on the opposite surface. The passage of the ethanol from one surface to the other indicated the presence of open cracks through the width of the material. These cracks and possibly the resultant oxidative loss of some of the matrix would cause a significant decrease in shear modulus. The permeability of PMR–15 specimens to ethanol after air aging is given in Table 2.

Stored moduli for PMR–15 and Avimid N composite plates (T–27 and AT–27) are presented in Fig. 9 and Table 3. The two specimens aged at 316 °C for 2090 hr were machined by cutting 1.5-mm-thick slices, progressing inward from one of the cut surfaces and parallel to the length dimension. DMA G' data for T–27 specimens (Fig. 9(a)) were taken for each slice. The data from the outer strips (slices l and 2) were significantly different from the data from the other strips and similar to the data shown for the T–89 specimen in Fig. 7(b). However, the data for slice 1 were lower than the T–89 data by two orders of magnitude. The G' data for slice 1 were also more than two orders of magnitude lower than values measured for slices 3 and 4, slices cut farther inward from the specimen

surface. Only a slight slope change occurs for slice 1 at what appears to be the T_G (470 °C, higher than the T_G for slices 3 and 4 (410 °C)).

An Avimid N composite specimen aged at 316 °C for 2090 hr was also sliced to provide samples for taking DMA data (Fig. 9(b)).

Only one significant difference explains the superior long-term thermo-oxidative stability performance of Avimid N composites in relation to other polyimides. For Avimid N (Fig. 9(b)) no great order-of-magnitude changes in G' occurred with distance from the molded surface as in the PMR–15 data (Fig. 9(a)). There was a slight increase in G' from slice 1 to slice 4 for Avimid N but not to the extent observed for the PMR–15. It appears that the outer surfaces of Avimid N were not degraded as much by oxidation as were the PMR–15 outer surfaces. The reason for this decrease in the magnitude of G' at the cut surfaces is addressed in the section Density and Void Content.

Glass Transition Temperature

The T_G data for T–5 specimens in Table 4 indicate that for aging temperatures at and below 260 °C the glass transition temperature was not dependent on either the aging temperature or the time at aging temperature under the conditions investigated. However, T_G increased at aging temperatures above 260 °C and also with aging time at 316 °C, the curing and postcure temperature for PMR–15. Although the specimens tested were all of the T–5 type, they were from four different plates fabricated separately. For the unaged materials T_G varied from 330 to 347 °C. The lowest T_G for unaged Avimid N was measured to be 359° C (not shown in table). No significant changes occurred in Avimid N after aging. For the Avimid N slices T_G remained constant as the distance of the slice from the edge of the plate increased. Also, T_G for the Avimid N composite was 20 to 40 deg C less than that for the PMR–15 composite after identical aging temperatures and times.

One might infer from these data that Avimid N undergoes little cross-linking. In comparison, the PMR–15 composite showed a wide range of T_G values as the material was examined from the outer surface inward. The brittle nature of PMR–15 composites is well documented, and the brittleness probably increases with high-temperature aging and increasing T_G.

Fiber Content

The fiber contents of both types of composite aged at 316 °C for 2090 hr were compared after cutting four slices of composite material from the edges of the two plates and digesting them in sulfuric acid. The results are presented in Table 5. In contrast to PMR–15 the outer two slices of the Avimid N laminate contained slightly less fiber than the inner two slices. The total gradient was somewhat less than 1% for both composite types. Fiber content did not decrease with distance for the PMR–15 composite.

Density and Void Content

Density measurements were made on similar edge slices of both the PMR–15 and Avimid N composites. The results are also listed in Table 5. The lower densities measured for the Avimid N slices reflect as much as 7% void content in the outer surface layer, 2% more than in the interior slices. The PMR–15 slices showed only slightly higher voids in the outer surface layer. The increase in porosity along the Avimid N cut surface exposed to the aging environment probably accounts for the decrease in the magnitude of the G' value in Fig. 9(b).

Microstructural Changes

Comparing the molded surfaces of the two types of polyimide composite indicated significant differences that may contribute to their long-term thermo-oxidative stability and mechanical property retention behavior. As previously noted and shown in Fig. 9, the outer 2.54-mm slice of the cut edge of the PMR–15 material had a G' value about two orders of magnitude less than that of the Avimid N material and the second PMR–15 slice. Slices 3 and 4 of the PMR–15 matrix composite and slices 2, 3, and 4 of the Avimid N composite had G' values of about the same magnitude. The reasons for the data spread are shown in Fig. 10. The cracks and absence of matrix material along the cut surface of the PMR–15 composite are evident. The tows with the fiber ends perpendicular to the plane of the paper contain cracks running between the fibers and perpendicular to the composite surface. The tows running parallel to the plane of the paper have regions of depleted matrix that appear as dark areas. These dark areas are cracks running parallel to the tows. Preparing a metallographic specimen by cutting the surface to be viewed at a 45° angle to both layers of tows gives a clearer picture of the

damage. Figure 11 shows this preparation for a specimen aged for 1730 hr at 316 °C. The cracks penetrated both layers of tows in the surface plies of the T650–35 fiber fabric. No void areas are visible in this figure. The inner volume of the PMR–15 composite was free of voids and cracks.

Figure 12 shows the cut surface of the Avimid N composite aged for 2090 hr at 316 °C at the position where the DMA specimens were cut. Two grooves made by the diamond wheel are visible at the top of the figure. Large voids are evident below the outer slice. The oxidative degradation probably removed matrix material from the surfaces of the voids that were originally exposed to the oven environment. This visual observation confirms the data in Table 5, which indicate a higher void content in the first slice of the Avimid N DMA specimens. Also, it is consistent with the lower G' value in the same slice shown in Fig. 10(b).

Figure 13 shows the Avimid N molded surface away from the inner diamond wheel slice visible at the top of Fig. 12. This surface was not directly exposed to the aging environment and is representative of the specimens tested in compression. The Avimid N outer molded surface had much less damage than the PMR–15 composite. In fact, no oxidative depletion of the matrix material, due to surface cracks, was observed in the outer plies. There were no signs that a distinct surface layer had formed. The slices were cut to measure about 2.54 mm thick.

Although the outer Avimid N surfaces appeared to have experienced little oxidation damage, the central volume of this composite had a heavy concentration of voids and cracks. We concluded from these data that, even though there was more thermal cracking in the Avimid N composite material than was seen in the PMR–15 material during 2090 hr of aging at 316 °C and the void content appeared to be excessive, the lack of visible signs of oxidative damage indicated that cracks and voids did not play a major role in the thermo-oxidative stability performance of Avimid N. Evidently, the matrix protected the reinforcement and the inner material from damage by the hostile environment. In addition to the microcracking, void formation and coalescence were observed at the matrix-fiber tow interfaces. The matrix actually separated from the fiber tows (Fig. 13) and the interfaces broke down. Coalescence and debonding were not present in the unaged specimen (Fig. 2). It can be concluded that this was due to thermal damage at the interface. This extreme degradation of

the Avimid N composite should be reflected in its mechanical properties after aging at high temperatures.

Compression Tests

One compression test was run on a straight-sided specimen from each of the two aged composites. These specimens were not machined to ASTM D–695 specifications. The specimens were cut from the edges of the two composites in the same manner as the dynamic mechanical analysis specimens. Thus, the two outer edges of the straight-sided specimens were the molded surfaces of the plate and contained the damaged molded surface layers. The measured strengths for the PMR–15 and Avimid N materials were 344.3 and 220.9 MPa, respectively. The corresponding moduli were 58.6 and 53.1 GPa. The average values of these two properties for three specimens of an unaged PMR–15 composite were 660.2 MPa and 68.7 GPa. The standard deviations were 13.9 MPa and 3.4 GPa, respectively (5). The PMR–15 composite lost 6.0% of its original weight and the Avimid N composite lost only 2.2%. Even though the PMR–15 lost three times as much weight as the Avimid N (since they both had the same nominal dimensions, they can be compared on a percentage basis), the Avimid N composite had a significantly lower retained strength than the PMR–15 composite.

Figure 14 [from (5)] shows the change in compression strength and modulus for T–5 PMR–15 specimens reinforced with the same type of fabric as the composites studied in this work. The specimens were aged at the five temperatures indicated in the figure. Except for the specimens aged at 204 °C, they all fall on a single curve when the compression strength is plotted as a function of percent weight loss. The compression strengths from this study are superimposed on the original figure. The PMR–15 data from this study fall in line with the data from (5), whereas the Avimid N data fall below the other data, in line with data measured for specimens aged at 204 °C.

Another set of specimens were cut from the T–27 and AT–27 plates aged at 260 and 316 °C for 20 000 and 2090 hr, respectively. They were machined as specified in ASTM D–695 so that the width directions were parallel with the molded surfaces of the plates (Fig. 15). The layers were removed in succession from the surface inward toward the center. Thus, the specimens were representative of the outer 9.1 mm of the plate material. Each layer was 2.54 mm thick.

Three of these T–27 and AT–27 layers oriented parallel to the molded surface were compression tested at room temperature for each condition (260 and 316 °C). The data are presented in Table 6. The retained properties were lower for the Avimid N composites than for the PMR–15 composites. The data from these tests are also plotted in Fig. 14 at 6.0 and 10.5% weight loss (PMR–15) and 0, 2.2, and 10.3% (Avimid N). The extension of the 204 °C curve, indicated by a dashed line, appears to have the same shape as the higher temperature data, but displaced downward.

It must be acknowledged that the ASTM compression test specimens did not contain two oxidized surface layers as did the straight-sided specimens described previously. Comparing the straight-sided specimen strengths with those of the ASTM D–695 specimens showed close agreement for Avimid N aged at 316 °C for 2090 hr. This result suggested that external oxidation was not a significant factor in strength retention for the Avimid N during aging. However, the large difference in strengths for the PMR–15 specimens suggested that the oxidized surface layers were a significant factor in strength retention for this composite.

Some data in Table 6 need explanation**.** The strengths and strains for the PMR–15 specimens aged at 260 °C for 20 000 hr had standard deviations and coefficients of variance much larger than those for the other specimens. The raw data showed 233.1 MPa for the strength of the outer specimen, 298.0 MPa for the second specimen (the second layer inward), and 264.6 MPa for the specimen farthest inside the aged plate. The outer specimen contained the thermally damaged molded surface layer with exposed fibers. This layer had lower values of strength and modulus. The data from test pieces cut farther in were more constant in magnitude.

A similar first slice was removed from the T–27 PMR–15 plate aged at 316 °C for 2090 hr. This slice, because of the severe matrix depletion, crumbled as it was being machined. A T–12 specimen was aged for 2090 hr at 316 °C, and the average measured compression strength was 462.9 MPa with a standard deviation of 20.8 MPa. The final thickness, as measured from the photomicrographs, was 89% of the original thickness. The calculated strength was 423 MPa. No such extreme differences in properties were evident in the Avimid N data.

In Fig. 16 [from (5)] PMR–15 material aged at 204 °C for 10 000 hr exhibited only slight signs of surface oxidation but did show excessive internal microcracking similar to the cracks observed in the Avimid N composite. The surface damage to the PMR–15 specimen significantly affected its compression properties. Although the cracks and voids in the Avimid N composite did not adversely affect the thermo-oxidative stability of that material, we concluded that they did degrade the mechanical properties. The extent of damage due to the voids alone was not determined in this study. However, the differences in the properties of the two materials at zero aging time may be due to the presence of the voids. In a previous study (12) it was shown that the interlaminar shear strength of unidirectional PMR–15 composite material decreased to approximately 80% of its void-free strength when it contained 5% voids. Therefore, it is not unreasonable to expect that similar effects could be observed with the compression strength.

COMPARISON WITH PREVIOUS WORK

Salin and Seferis (7) describe extensive work concerning the isothermal degradation of Avimid N neat resin and also 20- and 8-ply unidirectional and cross-plied composites reinforced with T–650, G30–500, and T–300 graphite fibers and aged at 371 °C. They noted the formation of voids along the exterior surfaces of Avimid N neat resin during aging. Also, they observed a lighter color along the outer surfaces of cut cross sections of the same specimens. Somewhat similar observations were made for the PMR–15 specimens in (13). In the present study void growth was observed along the cut edges of the Avimid N specimen aged at 316 °C for 2090 hr, but no light surface layers were seen at the temperatures investigated. Such layers may occur only above 343 °C for this material. Microcracking occurred throughout the core of the aged specimens and not just along the surfaces. Therefore, the cracking we witnessed probably was not due to voids.

Salin and Seferis (7) also calculated a 0.5 time exponent for weight loss flux during the initiation of aging (up to 300 hr), an indication that a diffusion-controlled mechanism prevails during this time. The aging temperature they studied is probably close to the processing temperature and may cause the release of residual reaction products that did not diffuse out at the lower temperatures. Avimid N aged at 371 °C may experience the onset of surface oxidation in a similar manner as PMR–15 aged at 270 °C.

Also, Salin and Seferis (7) observed a reaction zone at the fiber-matrix interface when the Avimid N composite was reinforced with G30–500 fibers. The zone appeared to be degradation of the fiber but not the matrix. The resulting weight loss was significantly greater for the G30–500-fiber-reinforced composite than for a T–300-fiber-reinforced laminate, probably due to the destruction of the interface in the former by fiber degradation. The degradation behavior of the Avimid N composite was similar to that of PMR–15 composites, which degrade more rapidly from the surfaces containing fiber ends (1) than from the molded surfaces. This behavior has been attributed to the breakdown of the fiber-matrix interface. The observations described in (7) agree with the details of the results reported herein.

DISCUSSION AND SUMMARY

The differences between the microcracking resistance and mechanical properties durability of the two different polyimides were unexpected a priori. The Avimid N composites experienced extensive microcracking during high-temperature aging. It was probably this microcracking, and not the internal void content, that was the primary cause of the lower compression properties for this condensation-curing polymer. This type of microdamage has been observed in PMR–15 composites with the identical fabric reinforcement when they were aged for more than 10 000 hr at 204 and 260 °C (5). The weight losses at these temperatures were about 0.4 and 4%, respectively. The high curing and postcure temperatures reported previously (8, 10, 11) may have aged the Avimid N past point A in Fig. 5. Therefore, the zero-weight-loss point was moved to the right and some compression strength was lost. These results suggest that all polymer-matrix composites processed at temperatures

above 316 °C should undergo long-term isothermal testing or suitable accelerated testing to monitor microstructural and mechanical property changes.

One other significant difference in the microstructures of the two types of composite was in their surfaces after aging. In Figs. 10 and 11 the molded and cut surfaces of the PMR–15 matrix specimen aged for 2090 hr at 316 °C contained a number of surface cracks and pronounced voids in surface layers that penetrated into the composite. However, the central volume showed no indications of either cracking or void formation. A more extensive description of this PMR–15 composite surface damage can be found in (5). It describes the high concentration oxygen levels in the surface layer and at the microcrack surfaces that extend into the composite. In contrast, the Avimid N composite showed no indications of oxygen concentration at the surfaces or around the microcracks and voids. The work of Salin and Seferis (7) suggests that such concentrations may occur at aging temperatures above 343 °C. However, extensive cracking occurred throughout the Avimid N specimen. Although Avimid N aging-induced dimensional effects were not addressed in this study, because of the variations in thickness across the specimens, we assumed that this polyimide experienced a minor size reduction during aging.

When the fiber volume contents and void volume contents were compared at different distances from the cut surfaces of the two types of specimen, little change due to position was evident. The data, presented in Table 5, reflect the large amount of void volume in the Avimid N composite and the absence of a volumetric gradient of fiber content as the distances from the cut surfaces increased. It is surprising that the Avimid N composite had higher measured fiber content than the PMR–15 material.

The relatively constant dynamic shear moduli G' and glass transition temperatures T_G as the Avimid N specimens were scanned across the thickness imply that their outer surfaces oxidized much less than those of the PMR–15 specimens. The surface degradation of the PMR–15 material was reflected in the changes in T_G and G' values as the specimen thickness was traversed.

These data illustrate the unreliability of using thermo-oxidative stability results to rate the extended thermal behavior of polymer-matrix composites. Both physical and mechanical property retention data are necessary to determine composite durability. They also demonstrate the detrimental effect of microcracking on the compression properties of polymer-matrix composites. Microstructural examination of all specimens is an important part of any study of thermal durability. It is not only necessary to determine what happens because of the environmental exposure, but it is more important to be able to reason why it happens.

REFERENCES

1. Bowles, K.J.; and Meyers, A.: Specimen Geometry Effects on Graphite/PMR–15 Composites During Thermo-oxidative Aging. Proceedings of 31st International SAMPE Symposium and Exhibition, 1986, pp. 1285–1299.
2. Bowles, K.J.; and Nowak, G.: Thermo-oxidative Stability Studies of Celion 6000/PMR–15 Unidirectional Composites, PMR–15, and Celion 6000 Fiber. J. Compos. Mater., vol. 22, Oct. 1988, pp. 966–985.
3. Magendie, F.J.: Thermal Stability of Ceramic and Carbon Fiber-Reinforced Bismaleimide Matrix Composites. M.S.E. Thesis, Univ. Washington, 1990.
4. Nan, D.J.; and Seferis, J.C.: Anisotropic Degradation of Polymeric Composites: From Resin to Composites. SAMPE Qtly., vol. 24, no. 1, 1992, pp. 10–18.
5. Bowles, K.J.; Roberts, G.D.; and Kamvouris, J.E.: Long-Term Isothermal Aging Effects on Carbon Fabric-Reinforced PMR–15 Composites: Compression Strength. ASTM STP–1302 (NASA TM–107129), 1997, pp. 175–190.
6. Scola, D.A.: The Status of High-Temperature Polymers for Composites—Likely Candidates. Proceedings of the 34th International SAMPE Symposium and Exhibition, 1989, pp. 246–258.
7. Salin, I.; and Seferis, J.C.: Anisotropic Degradation of Polymeric Composites: From Neat Resin to Composites. Polym. Compos., vol. 17, no. 3, June 1996, pp. 430–442.
8. DuPont NR–150 Polyimide Precursor Solutions. DuPont Product Information Pamphlet, 1976.

9. Meador, M.A.; Cavano, P.J.; and Malarik, D.C.: High Temperature Polymer Matrix Composites for Extreme Environments. Structural Composites: Design and Processing Technologies, Proceedings of the Sixth Annual ASM/ESD Advanced Composites Conference, ASM International, Materials Park, OH, 1990, pp. 529–539.
10. Gibbs, H.H.: Status Report: NR–150 Polyimide Binders and Adhesives. Proceedings of the 21st National SAMPE Symposium, 1976, pp. 592–606.
11. Avimid N Composite Materials. DuPont Product Information Pamphlet E–75102, 1987.
12. Bowles, K.J.: Long-Term Isothermal Aging Effects on Carbon Fabric-Reinforced PMR–15 Composites: Compression Strength. NASA TM–107129, 1996.
13. Bowles, K.J.; Jayne, D.; and Leonhardt, T.A.: Isothermal Aging Effects on PMR–15 Resin. SAMPE Qtly., vol. 24, no. 2, 1993, p. 2.

TABLE 1.—DIMENSIONS OF PMR–15 AND AVIMID N COMPOSITE SPECIMENS

Specimen	Length, cm	Width, cm	Thickness, cm	Weight, g	Percentage of edges
T–3	8.94	10.83	0.13	19.9	2.6
T–5	8.94	10.83	.25	40.7	5.4
T–12	8.94	10.83	.75	103.4	11.9
T–27	8.90	10.14	1.74	245.5	26.8
AT–27	9.44	9.46	1.79	225.6	27.5
T–89	10.13	.21	1.56	5.8	88.5

TABLE 2.—PERMEABILITY OF PMR–15 COMPOSITE SPECIMENS TO ETHANOL AFTER AIR AGING

Specimen	Aging time, hr	Aging temperature, °C	Weight loss, percent	Ethanol permeability
T–3	1510	316	10.00	None
T–9	1510	316	10.00	None
T–89	240	316	2.08	None
T–89	500	316	6.82	Full
T–89	860	316	13.19	Full
T–89	2000	260	2.46	Isolated wet spots on back surface
T–89	2000	288	4.28	Permeable with some isolated dry spots

TABLE 3.—GLASS TRANSITION TEMPERATURE AND STORED MODULUS OF PMR–15 AND AVIMID N COMPOSITE SPECIMENS

Specimen	Slice	Glass transition temperature, T_G, °C	Stored modulus, G', dyne/cm^2
T–27	1	465	1.3×10^{8}
	2	400	7.6×10^{9}
	3	409	2.2×10^{10}
	4	417	3.0×10^{10}
AT–27	1	374	1.0×10^{10}
	2	374	2.0×10^{10}
	3	370	2.0×10^{10}
	4	369	2.0×10^{10}

TABLE 4.—GLASS TRANSITION TEMPERATURES OF T–5 SPECIMENS AT DIFFERENT AGING TIMES AND TEMPERATURES

Aging time, hr	Aging temperature, °C				
	Room	204	260	288	316
0	330	– –	– – –	– –	– –
0	342	– –	– – –	– –	– –
0	347	– –	– – –	– –	– –
500	– –	– –	– – –	– –	358
1 000	– –	– –	– – –	349	364
2 000	– –	328	330	352	391
5 000	– –	323	– – –	346	– –
10 000	– –	322	349.5	– –	– –

TABLE 5.—FIBER CONTENT, VOID CONTENT, AND COMPOSITE DENSITY OF PMR–15 AND AVIMID N STRAIGHT-SIDED COMPRESSION TEST SPECIMENS

Matrix	Slice	Fiber content, vol.%	Void content, vol.%	Density, g/cm^3
PMR–15	1	57.6	0.8	1.5850
	2	59.6	–1.1	1.5944
	3	57.5	–.8	1.5843
	4	58.6	–1.0	1.5898
Avimid N	1	61.3	7.2	1.5314
	2	61.4	5.0	1.5523
	3	61.6	5.0	1.5554
	4	62.2	5.4	1.5554

TABLE 6.—COMPRESSION STRENGTH OF THREE OUTER LAYERS OF PMR–15 AND AVIMID N COMPOSITES

Characteristic	T–27 specimen			AT–27 specimen		
Aging temperature, °C	Room	316	260	Room	316	260
Aging time, hr	– – –	2090	20 000	– – –	2090	20 000
Strength, MPa	660.2	478.9	233.1	476.2	254.9	127.4
Standard deviation, MPa	13.9	7.0	84.6	28.6	32.1	24.4
Coefficient of variance, percent	– – –	1.5	36.6	6.0	12.6	19.1
Modulus, GPa	68.7	60.3	58.8	54.3	36.0	31.0
Standard deviation, GPa	3.4	1.4	2.2	2.8	2.2	3.5
Coefficient of variance, percent	– – –	2.3	3.5	5.2	8.9	7.1
Strain, percent	– – –	0.92	0.47	0.99	0.65	0.4
Standard deviation, percent	– – –	0.08	0.14	0.04	0.06	0.1
Coefficient of variance, percent	– – –	8.7	29.8	4.0	9.2	24.4

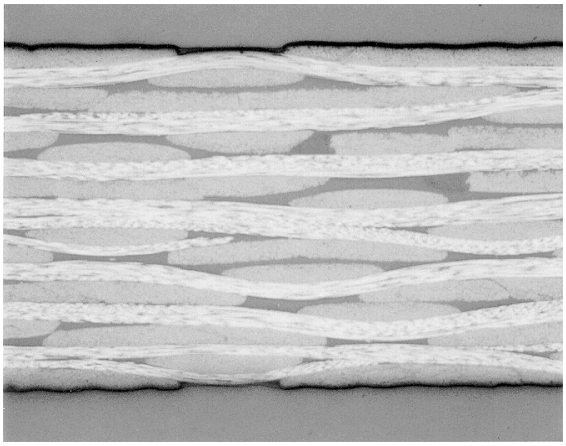

Figure 1.—Unaged T650–35-fabric-reinforced PMR–15 composite.

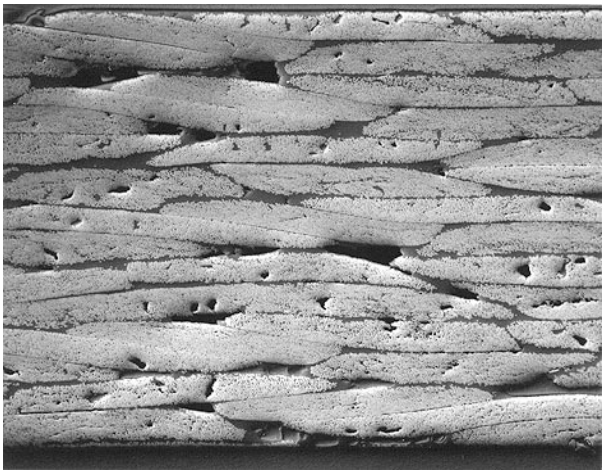

Figure 2.—Unaged T650–35-fabric-reinforced Avimid N composite.

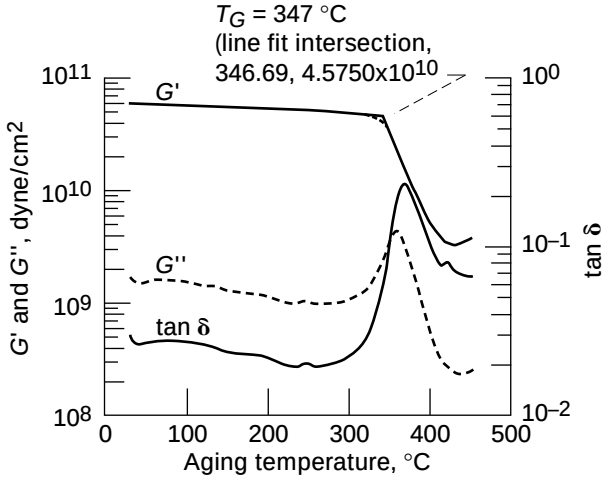

Figure 3.—Slope intersection as method for determining glass transition temperature. (Stored modulus *G*' curve is used for the measurement.)

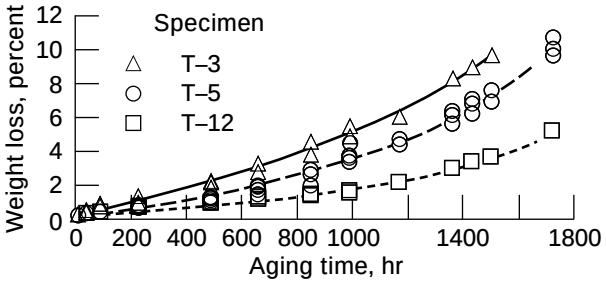

Figure 4.—Weight loss of PMR–15 composites as function of aging time at 316 °C.

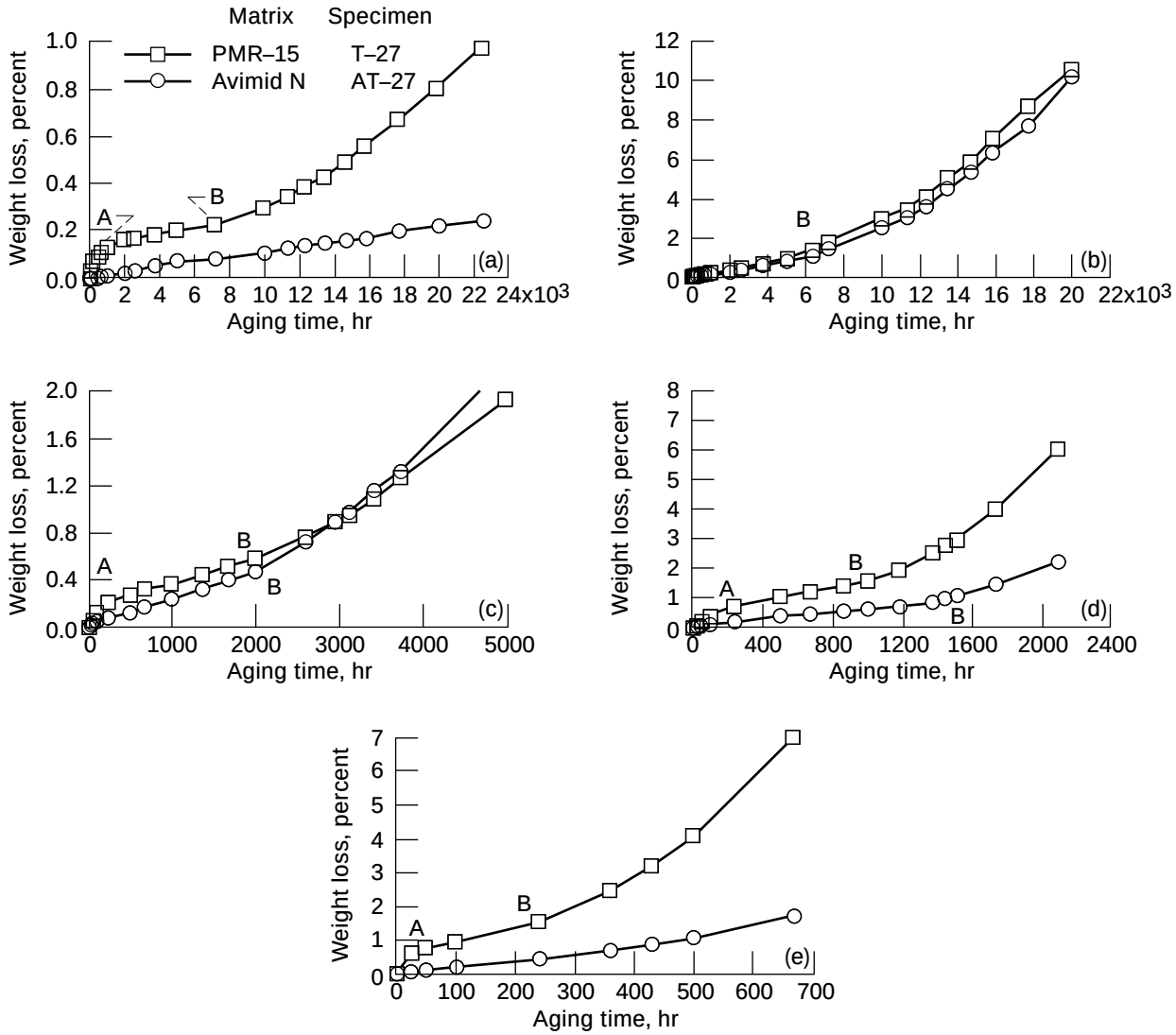

Figure 5.— Weight loss of PMR–15 and Avimid N composites at various aging temperatures as function of aging time. (a) 204 °C. (b) 260 °C. (c) 288 °C. (d) 316 °C. (e) 343 °C.

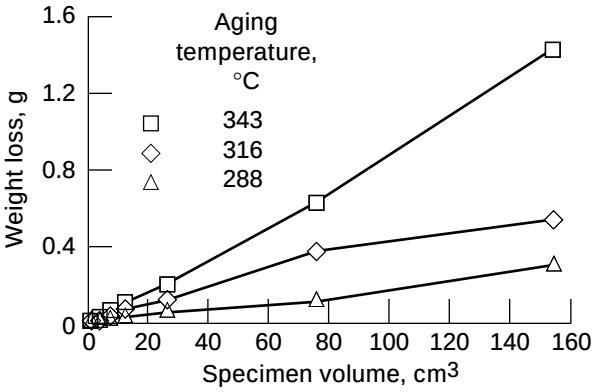

Figure 6.—Initial weight loss for PMR–15 composites as function of volume and aging temperature.

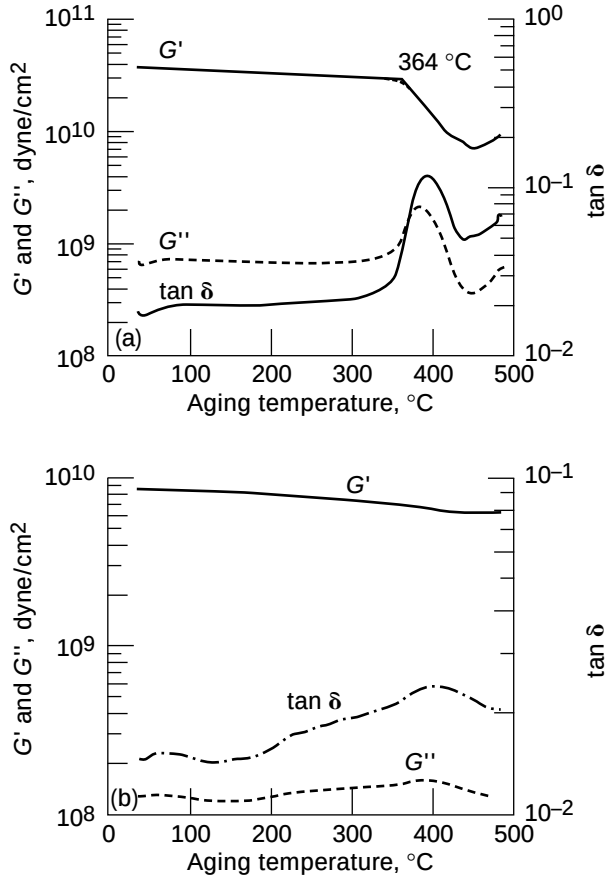

Figure 7.—Dynamic mechanical analysis data for PMR–15 composites aging at 316 °C for 1000 hr. (a) T–5 specimen. (b) T–89 specimen.

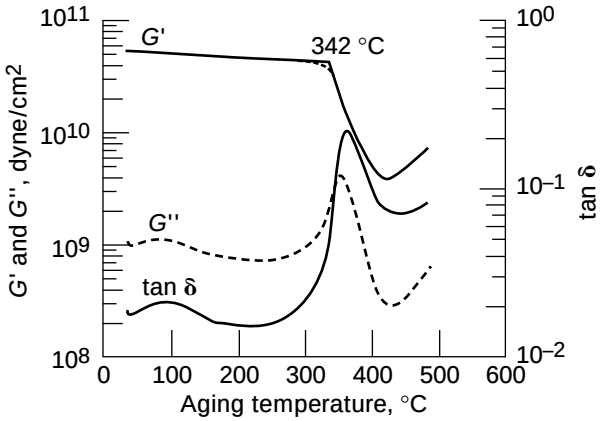

Figure 8.—Dynamic mechanical analysis data for T–89 PMR–15 specimen before aging.

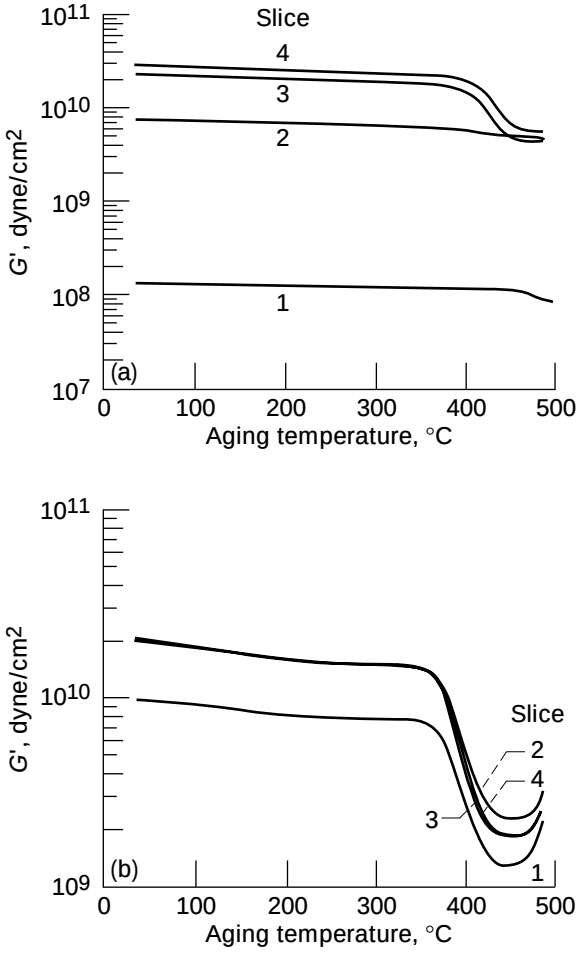

Figure 9.—Stored moduli of composites aged at 316 °C for 2000 hr. (a) PMR–15 (T–27). (b) Avimid N (AT–27).

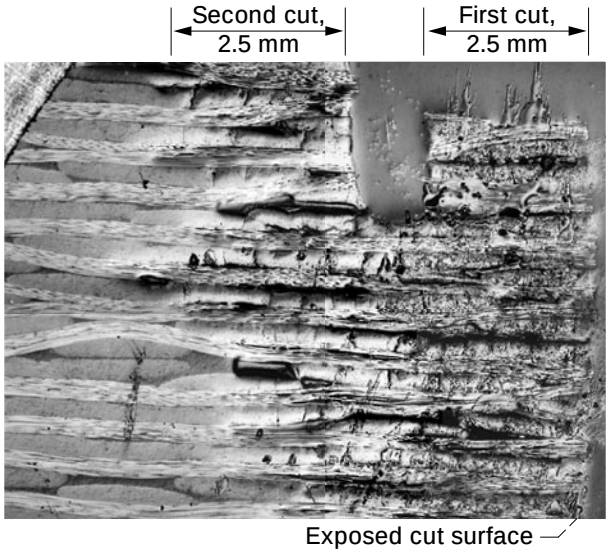

Figure 10.— T–27 PMR–15 composite aged at 316 °C for 2090 hr.

Figure 11.— PMR–15 specimen aged at 316 °C for 1730 hr and cut at 45° to show all fiber ends and cracking in both warp and fill tows.

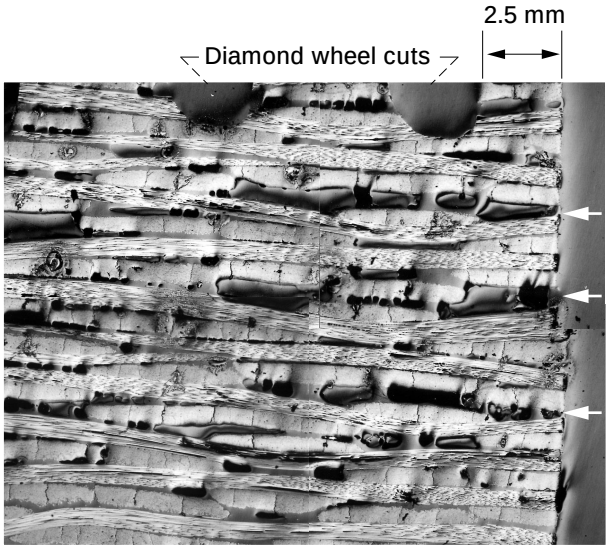

Figure 12.—Avimid N composite aged at 316 °C for 2090 hr. (Right surface is the cut edge exposed to the oven environment. Enlarged voids are indicated by arrows.)

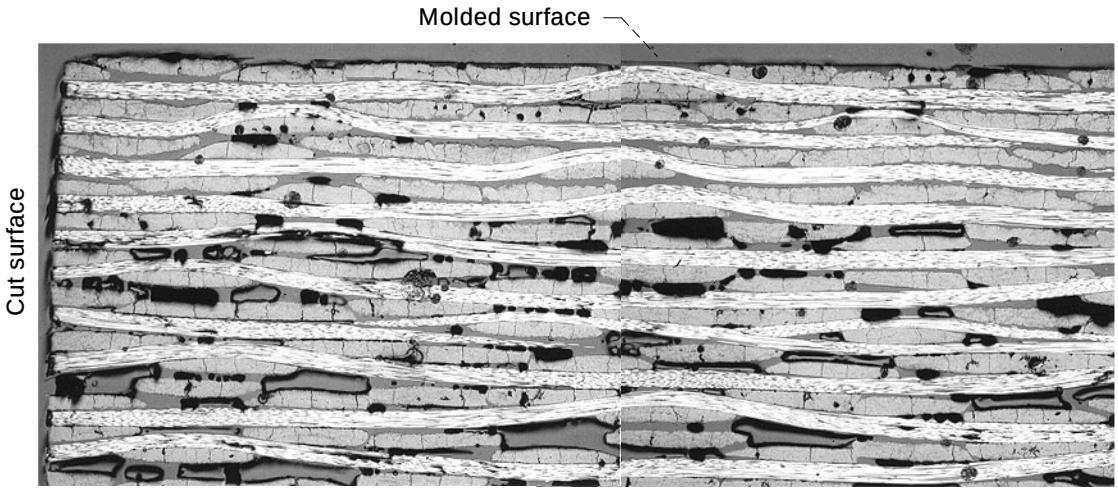

Figure 13.—Avimid N composite aged at 316 °C for 2090 hr, showing molded surface.

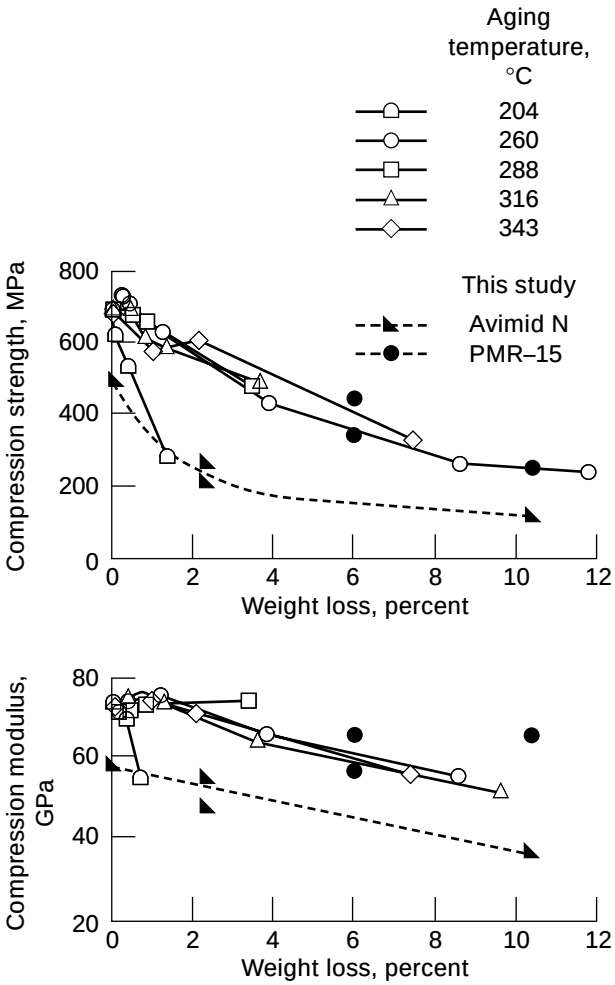

Figure 14.—Compression properties of aged PMR–15 composites.

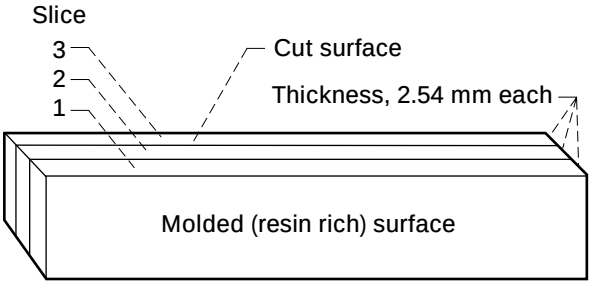

Figure 15.—Schematic for machining ASTM D–695 specimens for compression property tests.

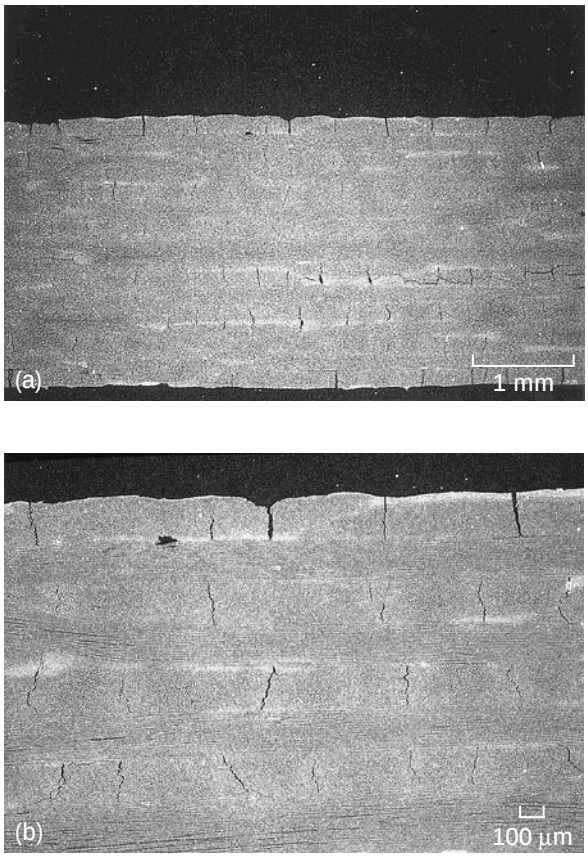

Figure 16.—Oxygen distribution in PMR–15 composite aged at 204 °C for 10 000 hr. (White areas are high oxygen concentration.) (a) Magnification, 20X. (b) Magnification, 100X.

REPORT DOCUMENTATION PAGE

Form Approved
OMB No. 0704-0188

1. AGENCY USE ONLY (*Leave blank*)	2. REPORT DATE	3. REPORT TYPE AND DATES COVERED
	February 1998	Technical Memorandum

4. TITLE AND SUBTITLE

Comparison of Graphite Fabric Reinforced PMR–15 and Avimid N Composites After Long Term Isothermal Aging at Various Temperatures

5. FUNDING NUMBERS

WU–538–06–15

6. AUTHOR(S)

Kenneth J. Bowles, Linda McCorkle, and Linda Ingrahm

7. PERFORMING ORGANIZATION NAME(S) AND ADDRESS(ES)

National Aeronautics and Space Administration
Lewis Research Center
Cleveland, Ohio 44135–3191

8. PERFORMING ORGANIZATION REPORT NUMBER

E–10847

9. SPONSORING/MONITORING AGENCY NAME(S) AND ADDRESS(ES)

National Aeronautics and Space Administration
Washington, DC 20546–0001

10. SPONSORING/MONITORING AGENCY REPORT NUMBER

NASA TM—1998-107529

11. SUPPLEMENTARY NOTES

Kenneth J. Bowles, NASA Lewis Research Center; Linda McCorkle and Linda Ingrahm, Gilcrest Electric, 3000 Aerospace Parkway, Brook Park, Ohio 44142 (work funded by NASA Contract NAS3–27351). Responsible person, Kenneth J. Bowles, organization code 5150 (216) 433–3197.

12a. DISTRIBUTION/AVAILABILITY STATEMENT

Unclassified - Unlimited
Subject Category: 24 Distribution: Nonstandard

This publication is available from the NASA Center for AeroSpace Information, (301) 621–0390.

12b. DISTRIBUTION CODE

13. ABSTRACT ***(Maximum 200 words)***

Extensive effort is currently being expended to demonstrate the feasibility of using high-performance, polymer-matrix composites as engine structural materials over the expected operating lifetime of the aircraft, which can extend from 18 000 to 30 000 hr. The goal is to develop light-weight, high-strength, and high-modulus materials for use in higher temperature sections of advanced 21st century aircraft propulsion systems. To accomplish this goal, it is necessary to pursue the development of thermal and mechanical durability models for graphite-fiber-reinforced, polymer-matrix composites. Numerous investigations have been reported regarding the thermo-oxidative stability (TOS) of the polyimide PMR–15 (1–5). A significant amount of this work has been directed at edge and geometry effects, reinforcement fiber influences, and empirical modeling of high-temperature weight loss behavior. It is yet to be determined if the information obtained from the PMR–15 composite tests is applicable to other polyimide-matrix composites. The condensation-curing polymer Avimid N is another advanced composite material often considered for structural applications at high temperatures. Avimid N has better thermo-oxidative stability than PMR–15 (6), but the latter is more easily processed. The most comprehensive study of the thermo-oxidative stability of Avimid N neat resin and composites at 371 ∞C is found in Salin and Seferis (7). The purposes of the work described herein were to compare the thermal aging behavior of these two matrix polymers and to determine the reasons for and the consequences of the difference in thermal durability. These results might be of some use in improving future polymer development through the incorporation of the desirable characteristics of both polyimides.

14. SUBJECT TERMS

Composites; Polyimides; Thermo-oxidative stability; Compression strength microstructure; Shear modulus

15. NUMBER OF PAGES

32

16. PRICE CODE

A03

17. SECURITY CLASSIFICATION OF REPORT	18. SECURITY CLASSIFICATION OF THIS PAGE	19. SECURITY CLASSIFICATION OF ABSTRACT	20. LIMITATION OF ABSTRACT
Unclassified	Unclassified	Unclassified	